Hydrogen Peroxide Generation by DC and Pulsed Underwater Discharge in Air Bubbles

Ranhua Xiong*, Anton Nikiforov, Patrick Vanraes, and Christophe Leys

Research Unit Plasma Technology (RUPT), Department of Applied Physics, Ghent University, Jozef Plateaustraat 22, B-900, Ghent, Belgium

Abstract:
The generation of H_2O_2 in underwater discharge in air bubbles is studied with consideration of the influence of electrodes polarity, input power, solution conductivity and the inter-electrode distance. The efficiency of hydrogen peroxide generation strongly depends on the polarity, input power and the inter-electrode distance. Discharges in air bubbles with water as a cathode have significantly higher energy yield of hydrogen peroxide in comparison with negative DC or pulsed discharges. The generation of hydrogen peroxide by DC discharge increases with decrease in the inter-electrode distance, but it is opposite for pulsed discharges. Different efficiency of H_2O_2 production is explained based on physical processes which result to formation of OH radicals.

Keywords: Hydrogen peroxide generation; Underwater discharge; Atmospheric plasma

Introduction

Over the past years, underwater electrical discharges have received a lot of attention in view of possible applications in different fields of science and technologies such as advanced oxidation of water pollutions, sterilization, organic synthesis (1-3). Underwater discharges can be used as a source of active species (O_3, OH, O_2^*, H_2O_2), ions (H_3O^+, O^+, H^-, O^-, OH^-), UV radiation and shock wave (4-5, 39). It is clear that these high reactive species produced in liquid medium can be used to degrade many organic compounds, for sterilization, water purification, etc. (6, 7, 40). There are a lot of methods by which underwater plasma can be generated and sustained. In general, underwater discharges can be divided into three main groups based on the physics of underwater breakdown (8). Streamer/spark discharges in a gas and liquid medium are always generated by high voltage pulsed with duration from a few nanoseconds to microseconds with the current up to some kA (43). The second group of underwater discharges is diaphragm or capillary discharge where two reservoirs filled with a conductive liquid are separated by a dielectric barrier in which a current pathway (diaphragm) is made between two reservoirs or water streamers (16, 37). The plasma is formed in the pathway by AC or DC high voltage across the reservoirs. The third group is electrical discharges in gas or vapor bubbles or on the water surface (18, 41, 42). Different kinds of experimental setups developed for discharge in gas or vapor bubbles were summarized in a recently published review article (9). One of the types is a discharge in bubbles which are produced by external gas flow through a glass tube in which a metal high voltage electrode is inserted. This type of reactor with artificially produced bubbles has an advantage of significantly reducing of the input power because of absence of Joule heating of liquid medium. Additionally, this discharge can be initiated by DC voltage with much lower voltage compared to direct liquid phase discharge (10-11). Reducing the rate of erosion of electrode is another advantage of this type of reactor. Presence of plasma/liquid interface allows initiating of a wide range of chemical reactions in gas phase as well as in a liquid medium. Most of the researcher revealed direct correlation of plasma-liquid treatment efficiency (purification, sterilization, etc.) with amount of H_2O_2 produced by plasma. Hydrogen peroxide formation by means of plasma is useful indicator for commercial applications in chemical, environmental and disinfection processes (14-15). A recent review (13) on hydrogen peroxide formation in electrical discharge plasma with liquid water shows major factors affecting hydrogen peroxide formation in gas and liquid. Among of them are: UV radiation, temperature, ozone, pH, solution conductivity, salt type and electrode materials.

The present study is focused on the hydrogen peroxide formation in DC and pulsed discharge and on the effect of input power, solution conductivity, inter-electrode distance and water polarity on hydrogen peroxide formation. In order to estimate the efficiency of hydrogen peroxide formation by the reactor, the energy yield and generation rate of hydrogen peroxide are compared with literature.

*Corresponding author; E-mail: Ranhua.Xiong@UGent.be

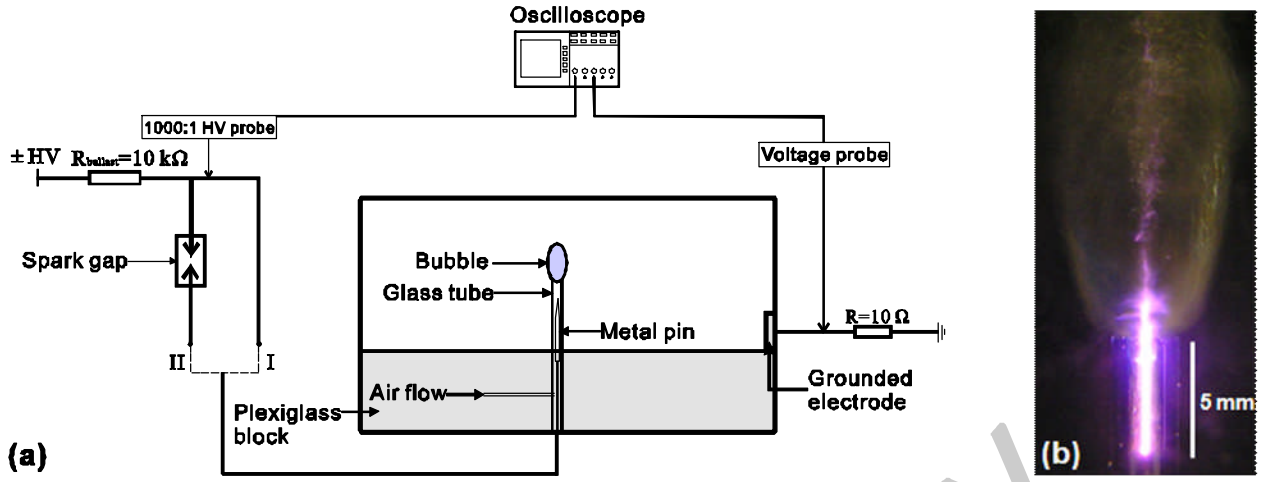

Figure 1. (a) Experimental set-up: underwater discharge in air bubbles generated by DC (I) or pulsed voltage(II); (b) an image of positive DC discharge plasma with the inter-electrode distance d=5 mm, current I=30 mA, solution conductivity σ=250 μS/cm.

Experimental Set-up

The scheme of the reactor is shown in Figure 1. The discharge is generated in the air bubbles between a metal pin positioned inside of glass tube and the water surface. In present study positive and negative DC power supply and pulsed generator have been used in order to generate plasma. The DC discharge is excited by positive or negative voltage through a ballast resister (10 kΩ) in the range of 1-3 kV and current of 10-40 mA. The pulsed discharge is produced by means of self triggered spark gap stabilized by fast gas flow. Air flow applied for stabilization of the pulsed generator is used furthermore for bubbles production by subdivision of air flow into 14 channels. Each tube is connected to a glass tube at one side of the Plexiglass block used as a reactor vessel. The metal needle-pins inside of the glass tubes at the bottom of vessel play the role of a high-voltage electrode. The distance from the tip of pin to the orifice of glass tube is adjustable. The distance is also regarded as inter-electrode distance. It has to be noted that although the reactor can sustain plasma in 14 independent channels at average current of 30 mA in pulsed mode, only one channel is used in case of DC mode because of current limitation of the power supply. The grounded electrode is a metal tube placed at one side of the vessel as shown in Figure 1. All experiments are carried out in a solution of $NaH_2PO_4.2H_2O$ with initial conductivity 50 or 1500 μS/cm. Tektronix P6015A 1000:1 high voltage probe is used to measure the applied voltage waveform. The solution conductivity in the vessel is measured by Consort C533 meter.

The concentration of hydrogen peroxide in the liquid produced by the discharge is determined with a photometric method using the reactions of H_2O_2 with metavanadate ammonium as explained in detail in (17). Used method has almost the same sensitivity and selectivity to H_2O_2 as a reaction with titanium (IV) oxalate (30) and an advantage of long life time of reagents. The statistic error of measurement is estimated about 5% for H_2O_2 concentration higher than 5 mmol/L and 10% for lower concentration (19).

Results and Discussion

Electrical Properties of DC and Pulsed Discharge

Voltage/current (V/C) characteristics of DC discharge and typical current-voltage waveforms of pulsed discharge in bubbles are presented in Figure 2. Figure 2 (a) is corresponding to the positive DC discharge at 2 mm inter-electrode, 50 μs/cm initial conductivity. Visual appearance and V/C characteristics of DC discharge are similar to one investigated by Bruggeman P. et al (31) whereas the pulsed mode of the discharge has not been used and reported before. It has to be noted that in the present work we do not provide more details on physical properties of the discharge like n_e, T_e, spectral characteristics because of our focus on estimation of chemical efficiency of the plasma and the very complex relation between plasma properties and rate of H_2O_2 production. The power of DC and pulsed discharge is defined as follow and is used furthermore for estimation of hydrogen peroxide yield:

$$P = \bar{U}\,\bar{I} \qquad P = \frac{1}{\Delta T}\int_{T}^{T+\Delta T} U(t)I(t)dt \qquad [1]$$

where $\bar{U}$, $\bar{I}$ are average voltage, current of DC discharge and $U(t)$, $I(t)$ are voltage and current during time of ΔT for pulsed discharge.

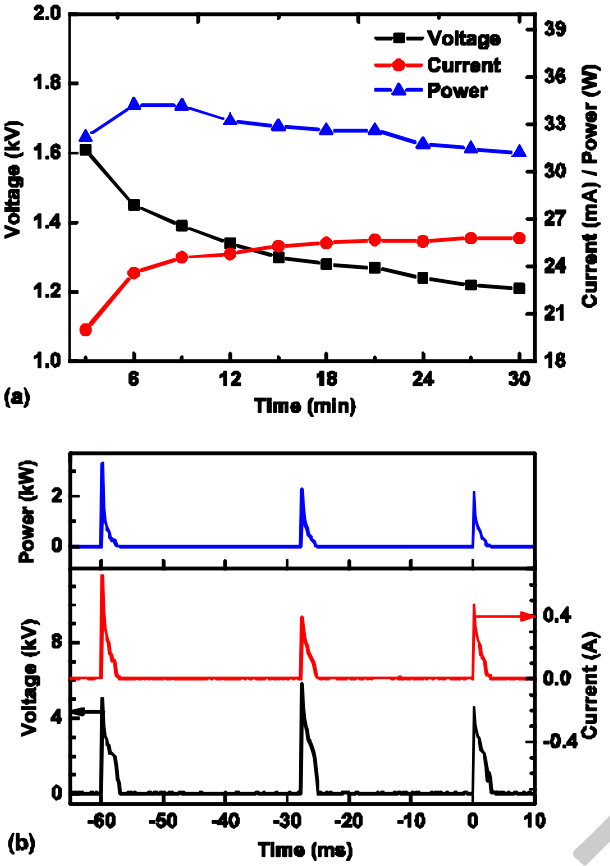

Figure 2. Voltage, current and power characteristics of positive DC discharge (a) and voltage-current waveform of positive pulsed discharge (b) at inter-electrode distance d=2 mm and initial conductivity σ=50 μS/cm.

During DC operation the average voltage decreases from 1.61 kV at beginning to 1.22 kV after 30 min, and the average current increases from 20 mA to 26 mA while the power is nearly constant at 32 W as shown in Figure 2 (a). The negative DC discharge has similar electric features. The main reason is the increase of solution conductivity from 50 μS/cm to 1100 μS/cm after 30 min due to the formation of HNO_3 in solution under plasma action (20). The voltage change can be explained by the change in the equivalent resistance of the water electrode with time. The equivalent resistance is nearly 10 kΩ in initial water with conductivity of σ=50 μS/cm, while it is only several hundreds Ω at the end of the experiment for the conductivity of 1 mS/cm and so the corresponding voltage drop changes from hundreds volt to several volts. Figure 2 (b) represents the positive pulsed discharge voltage and current waveform. Although the conductivity increased approximately to 330 μS/cm, the pulsed discharge is unaffected by conductivity change like DC discharge. The increase of the discharge current (peak value) in pulsed mode from 0.6 A to 0.65 A is observed after 30 minutes of discharge operation which results to slight increasing the discharge power on 7-10% at the end of the experiments. No difference in shape of current or voltage pulses has been observed in pulsed plasma due to change of the solution conductivity.

Hydrogen Perxiode Generation with Different Polarity and Conductivity

Hydrogen peroxide is generated in reactor in a large number of reactions (5, 14, 16). Reduced set of reactions of H_2O_2 formation and destruction on the basis of the literature data is presented in Table 1.

The H_2O_2 generation by other particles such as OH^-, H^+, HO_2, and O^{*-} is negligible in the view of their low concentration in the solution and there are not presented in Table 1 (27, 38). Based on results of some recent calculations (13) and investigations of mechanisms of (27) underwater discharge chemical efficiency, the main H_2O_2 production path is generation from OH radicals in dimerization reaction - Table 1 reaction 3. Because of key role of OH radical in the plasma chemistry of the underwater plasma in air bubbles the set of reactions of OH radical production can be written as (with k in cm^3s^{-1}):

Electron collisions

$e + H_2O \rightarrow OH + H + e$
$k=2.3\times10^{-12} - 1.8\times10^{-10}$ T_e = 1–2 eV (34)

$e + H_3O^+ \rightarrow OH + H_2 + e$
$k=10^{-6}$ T_e = 1 eV (34)

$e + H_2O \rightarrow OH + H^-$
$k=4.9\times10^{-12}–4.7\times10^{-11}$ T_e= 1–2 eV (34)

Ion collisions

$H_2O^+ + H_2O \rightarrow OH + H_3O^+$ $k=1.9\times10^{-9}$ (27)

Dissociation by radicals and metastables

$N_2(A) + H_2O \rightarrow OH + N_2(X) + H$
$k=6\times10^{-14}$ $T_g \approx 300K$ (34)

$N(^2D) + H_2O \rightarrow OH + NH$
$k=2.5\times10^{-10}$ $T_g \approx 300K$ (34)

$O(^1D) + H_2O \rightarrow OH + OH$
$k=2.2\times10^{-10}$ $T_g \approx 300K$ (27)

$O + H_2 \rightarrow OH + H$
$k=9.3\times10^{-18}–5.7\times10^{-11}$ Tg = 300–3000K (35)

$H + O_2 \rightarrow OH + O$
$k=2.5\times10^{-21}–1.3\times10^{-11}$ T_g = 300–3000K (35)

Vibrational collisions

$H_2O + H_2O^* \rightarrow OH + H + H_2O$
$k=10^{-14}$ T_v = 0.5 eV T_g = 300K (35)

Table 1. Rate of reactions of H_2O_2 formation and destruction under plasma action in cm^3s^{-1} for two-body reactions and cm^6s^{-1} for three-body reactions.

N	Reaction	Typical rate	Reference
1	$HO_2 + HO_2 \rightarrow H_2O_2 + O_2$	$2.2x10^{-13}e^{600/T}$	[33]
2	$HO_2 + HO_2 + M \rightarrow H_2O_2 + O_2 + M$	$1.9x10^{-33}e^{980/T}$	[33]
3	$OH + OH + M \rightarrow H_2O_2 + M$	$2.6x10^{-11}$ at 298 K	[33]
4	$H_2O_2 + O \rightarrow HO_2 + OH$	$1.4x10^{-12}e^{-2000/T}$	[33]
5	$H_2O_2 + OH \rightarrow HO_2 + H_2O$	$2.9x10^{-12}\ e^{-160/T}$	[33]
6	$H_2O_2 + e \rightarrow OH + OH + e$	$2.36x10^{-9}$	[32]
7	$H_2O_2 + e \rightarrow H + HO_2 + e$	$3.1x10^{-11}$	[27]
8	$H_2O_2 + H \rightarrow H_2 + HO_2$	$8.0x10^{-11}\ \exp(-4000/T_g)$	[27]
9	$H_2O_2 + H \rightarrow H_2O + OH$	$4.0x10^{-11}\ \exp(-2000/T_g)$	[27]
10	$H_2O_2 \rightarrow 2OH$	$2x10^9 T_g^{-4.86}\ \exp(-26821/T_g)$	[27]

Table 2. Rate of reactions of OH destruction and quenching in presence of N_2 and O_2.

N	Reaction	Typical rate (cm^3s^{-1})	Reference
1	$2OH \rightarrow O + H_2O$	$1.8x10^{-12}$	[36]
2	$OH + H_2 \rightarrow H + H_2O$	$7.7x10^{-12}\ \exp(-2100x8.6x10^{-5}/T_g)$	[36]
3	$OH + O \rightarrow H + O_2$	$2.3x10^{-11}\ \exp(-110x8.6x10^{-5}/T_g)$	[36]
4	$OH + O \rightarrow HO_2$	$2.1x10^{-10}$	[32]
5	$OH + O_3 \rightarrow HO_2 + O_2$	$1.9x10^{-12}\exp(-1000x8.6x10^{-5}/T_g)$	[32]
6	$OH + H \rightarrow H_2O$	2×10^{-10}	[34]
7	$OH + HO_2 \rightarrow H_2O + O_2$	$1.1x10^{-10}$	[28]
8	$OH + N \rightarrow O + NH$	$4.7x10^{-11}$	[34]
9	$OH + NH \rightarrow NO + H_2$	$8x10^{-11}$	[34]
10	$OH + HNO \rightarrow NO + H_2O$	$1.5x10^{-11}$	[34]
11	$OH + NO + M \rightarrow HNO_2 + M$	$3.3x10^{-11}$	[34]
13	$OH + NO_2 + M \rightarrow HNO_3 + M$	$7.5x10^{-11}$	[34]

Thermal dissociation starts to play an important role if T_g higher than 2500 K that can be realized e.g. in cathode area of the discharge:

$$H_2O + H_2O \rightarrow OH + H + H_2O$$
$$k=10^{-20}–4x10^{-14}\ cm^3s^{-1} \quad Tg=2500–5000K \qquad (34)$$

The set of reactions of OH destruction is presented in Table 2. In order to take in to account effect of air in our system some important reactions including nitrogen chemistry are included in Table 2 as well. Generation of plasma in air buubles leads to generation of ground state OH in reactions of H_2O dissociation as shown above with rate constant as high as $2.5x10^{-10}\ cm^3s^{-1}$, but on the other hand OH radicals effectively reacts with nitrogen oxides NO and NO_2, Table 2 reactions 10-11, as well as with NH, HNO and N. From technological point of view it is important to mention that sustainment of the discharge in air bubbles leads to acidification of the solution due to formation of HNO_3.

The global kinetic of hydrogen peroxide production and decomposition can be assumed to follow zero-order kinetics at initial time at shown on Figure 3 and can be describe as :

$$\frac{d[H_2O_2]}{dt} = k_1 - k_2(T)[H_2O_2] \qquad [2]$$

where $[H_2O_2]$ is the hydrogen peroxide molar concentration, k_1 is the H_2O_2 production rate constant, k_2 is the decomposition rate constant. The main reaction leading to the formation of H_2O_2 by discharge in air bubbles is dimerization of OH radical whereas decomposition is mainly due to thermal destruction as follows (20, 26):

$$H_2O_2 \xrightarrow{K_2(T)} H_2O + \frac{1}{2}O_2 \qquad [3]$$

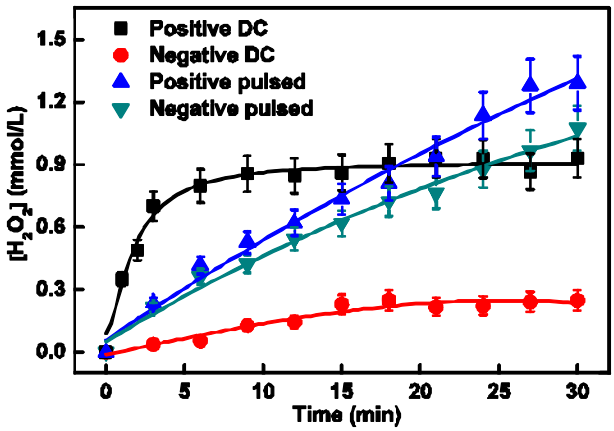

Figure 3. Hydrogen peroxide generation with time by positive, negative DC (P=45 W d=2 mm, σ=50 μS/cm) and pulsed discharge (P=40 W, d=2 mm, σ=50 μS/cm).

Figure 3. shows experimental results on the H_2O_2 generation over time by positive, negative DC and pulsed discharge in air bubbles. The H_2O_2 generation by positive DC discharge (water as cathode) reaches a steady-state condition after about 300 s as shown in Figure 3 at a H_2O_2 concentration of 0.7 mmol/L. At steady-state regime observed in experiemts, the rate of H_2O_2 destruction (depending on k_2) is equal to the rate of formation (depending on k_1) which means that thermal destruction of H_2O_2 plays an important role in DC mode. For negative DC discharge (water as anode), the H_2O_2 concentration is much lower, not more than 0.2 mmol/L after 30 minutes of the discharge. Similar results on influence of polarity has been mentioned in (20). The H_2O_2 concentration linearly increases over time during 27 min and then reaches a steady-state mode on time scale of 60-70 minuts for pulsed discharges. The H_2O_2 generation rate of positive pulsed discharge is slightly higher by comparsion with negative pulsed discharge.

According to our experimental results the solution conductivity has a negligible influence on H_2O_2 formation where the reason is that the discharge within bubbles in liquid is generated in a gas phase and mechanism of H_2O_2 generation is not effected by solution conductivity.

Hydrogen Peroxide Generation with Different Input Power and Different Inter-electrode Distance

Kinetic plots of the H_2O_2 concentration for different input power at fixed inter-electrode distance of 2 mm and initial conductivity of 50 μs/cm are presented in Figure 4(a) for positve DC discharge and figure 4(b) for negative pulsed discharge. Increase of the input power in pulsed discharge results in the growing of

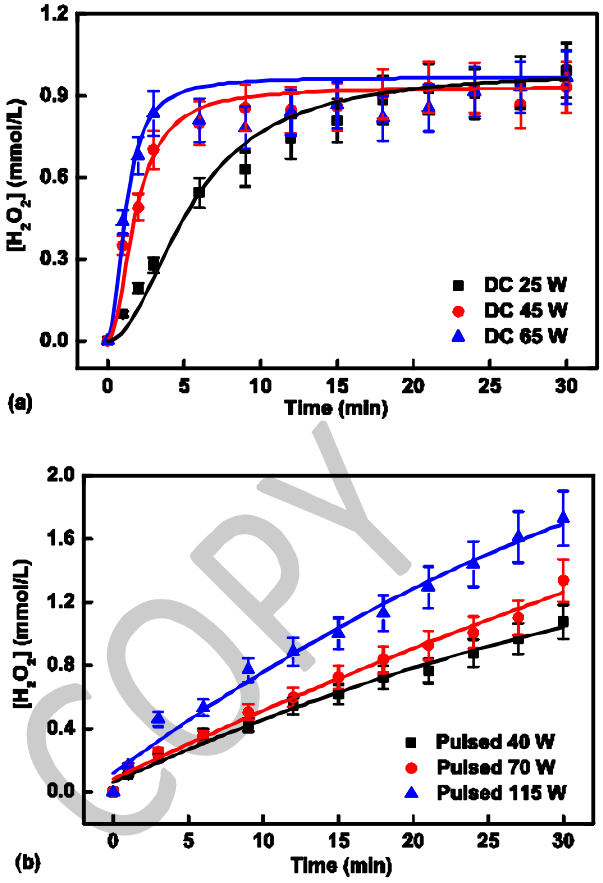

Figure 4. Hydrogen peroxide generation with time by positive DC ((a) σ=50 μS/cm, d=2 mm) and negative pulsed ((b) σ=50 μS/cm, d=2 mm) discharge with different power.

H_2O_2 concentration with almost linear dependence on input power. Whereas an increase of the input power from 25 to 65 W of DC discharge leads to almost the same steady-state concentration of H_2O_2 but the initial slope of the kinetic plots has a strong dependence on input power. Probably the main explanation is the thermal destruction of H_2O_2 in case of DC discharge where gas temperature directly depends on the input power (8-9). In order to take into account the process of H_2O_2 destruction, it is necessary to calculate the energy yield of H_2O_2 formation to estimate the efficiency of H_2O_2 generation. The H_2O_2 formation energy yield has been calculated from initial formation rate as (16):

$$h_{H2O2} = \frac{dC_{H_2O_2}}{dt}\Big|_{t\to 0} \cdot (t_2 - t_1) \cdot Mr(H_2O_2)P^{-1} \quad [4]$$

where t_2-t_1=3600 s, $Mr(H_2O_2)$ is the molecular mass of H_2O_2, P (defined in (1)) is the power of the discharge, $dC_{H_2O_2}/dt|_{t\to 0}$ is the initial rate of H_2O_2 formation, which can be calculated from the slope of the initial linear section of the kinetic curves.

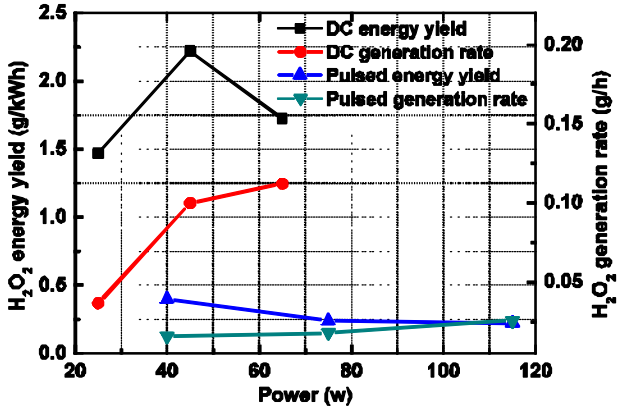

Figure 5. Hydrogen peroxide energy yield and generation rate with different power for positive DC and negative pulsed discharge corresponding to Figure 4 (a) and (b).

Figure 5 shows the H_2O_2 energy yield and generation rate at different power of DC and pulsed discharge. Although the H_2O_2 generation rates increase with higher power, the H_2O_2 energy yields have different characteristics. It can be seen from Figure 5 that the H_2O_2 energy yield of DC discharge goes through a maximum (2.22 g/kWh), after which, with a further increase in power, starts to decrease. On the other hand, the energy yield of pulsed discharges is almost constant at different power and much smaller than one for DC dischagre.

Another important parameter of the plasma/liquid system is the inter-electrode distance, which has strong influence on H_2O_2 production (12, 22, 23). Figure 6 shows the production of hydrogen peroxide by DC (a) and pulsed (b) discharges at different inter-electrode distances. The kinetic plots of hydrogen peroxide generation in DC discharge follow equation [8] with high $k_2(T)$ at 2 and 4 mm inter-electrode distance. During the first phase (the first 3 min discharge as shown in Figure 6 (a)), the hydrogen peroxide concentration is nearly linear increase with time at different inter-electrode distance. After the first 3 min, the hydrogen peroxide concentration increases with a lower rate by comparison with the first phase at inter-electrode distance of 1 mm, while it reaches a steady-state at the inter-electrode distance of 2 mm. H_2O_2 concentration almost linearly decreases with time after first phase when the inter-electrode distance is set as 4 mm. An explanation of the effect is the thermal destruction of H_2O_2 in the water near the air-water interface. Estimation of the gas temperature from emission of the N_2 band (not shown here) gives gas temperature about 2300±150 K for 1 mm distance and 3500±150 K for 4 mm distance. Validity of used method for gas temperature measurements has been proved by numerous works; see e.g. (8) and references

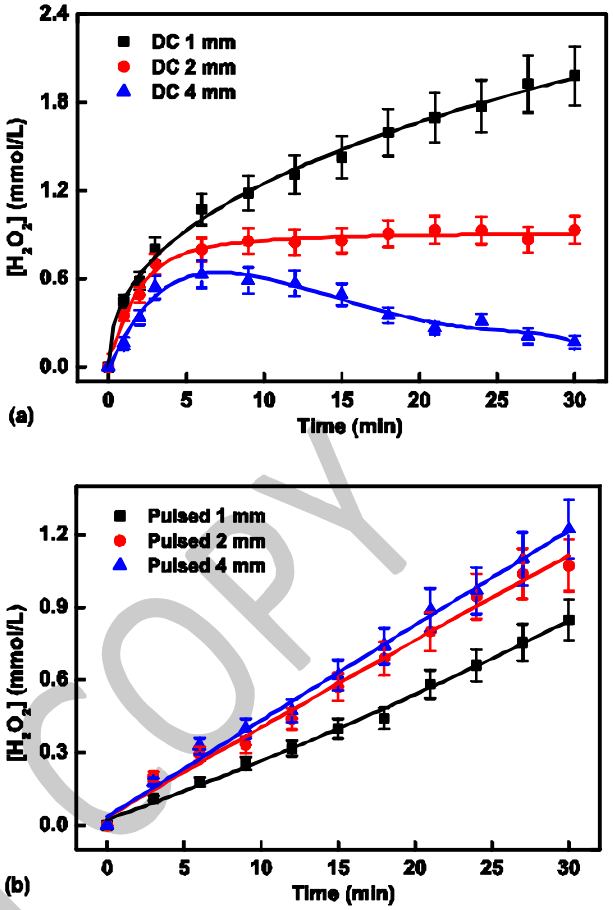

Figure 6. Hydrogen peroxide generation with time by positive DC (P=45 W, σ= 50 μS/cm) and negative pulsed discharge (P=65 W, σ=50 μS/cm) at different inter-electrode distance.

herein. Because of the increasing residence time and gas temperature with increase of the inter-electrode distance, more energy transfers to the bulk water in the vicinity of the air-water interface during plasma operation. This leads to almost linear increase of liquid medium temperature with increase of the electrode gap. On the contrary with DC discharge, the hydrogen peroxide generation rate increases with increasing inter-electrode distance in the case of pulsed discharge which is characterized by a much lower gas temperature around 1500±150 K not depending on the gap size.

In view of applications it is worthwhile comparing different types of discharge based on the efficiency of the hydrogen peroxide formation. The data of the maximum energy yield are listed in Table 3. It has to note that the energy yield values in case of pulsed mode are almost independent on the applied voltage. In case of interest to other plasma/liquid systems we would like to refer readers to the recent review by B. Locke (13) where extensive comparison of different systems is presented.

Table 3. Hydrogen peroxide generation energy yields and generation rate by using negative, positive DC and pulsed power.

Discharge mode and polarity	Input power (W)	Energy yield (g/kWh)	Generation rate (g/h)
Positive DC	45	2.30	1.04E-1
Negative DC	45	0.22	9.79E-3
Positive Pulsed	40	0.60	2.50E-2
Negative Pulsed	40	0.40	1.59E-2

It can be stated, based on the presented results, that the H_2O_2 energy yield is higher when water is a cathode. As discussed previously, the main reaction of H_2O_2 generation is dimerization of solvated OH radicals in liquid phase – Table 1, reaction [3]. OH radical is produced under plasma action in a wide set of processes but furthermore it effectively reacts with H_2O, N_2 and O_2, etc. see e.g. (27-28). Characteristic life time of OH radical because of quenching and its high reactivity is in the order of 10^{-7} s which means that only OH radicals produced on the plasma/liquid interface with μm thickness can reach the liquid, be solvated and take a part in Table 1, reaction [3]. This condition is realized in streamer pulsed discharge (4-5) with duration of exciting pulse up to 10^{-6} s produced directly in liquid and in the cathode or anode layer of DC glow discharge in gas bubbles (29). In case of glow discharge, the density of OH radicals is higher in the cathode layer (water as a cathode) than in anode region (water as a anode) because of much higher input energy dissipated in the former ($I_{discharge}$*cathode fall), high density of water vapor by compare with gas phase and high gas temperature around 5000-7000 K where water thermal dissociation starts to play important role in OH production (8, 31). It is found that the hydrogen peroxide energy yield by positive DC discharges in air bubbles is nearly two times higher than the values reported for DC discharges in liquid and for discharges over the liquid (13). The reasons of low efficiency of pulsed system used in present work are considerably long duration of pulses and streamer mode of the discharge in gas phase. Pulsed plasma shows the absence of a glow structure and no distinguishable cathode region responsible for OH production. Correspondingly, only very few OH radicals produced in gas phase can reach liquid phase that explains so low yield of H_2O_2 in pulsed plasma here and from similar system used by other groups (12, 25).

Conclusion

Chemical efficiency of underwater DC and pulsed discharges in air bubbles is characterized by measurement of H_2O_2 production. The effect of polarity, input power, solution conductivity and the inter-electrode distance is investigated and discussed for both discharge configurations. Discharge with water as a cathode is much more effective for H_2O_2 production. The energy yield of hydrogen peroxide in DC positive discharge is as high as 2.30 g/kWh but only 0.22 g/kWh for negative DC discharge. The highest hydrogen peroxide energy yield in case of pulsed discharge is only 0.4 g/kWh, and input power has negligible influence on it. With comparison of hydrogen peroxide energy yield of present reactor and literature data, it is found that the discharge in air bubbles sustained by positive DC power has the highest efficiency because of presence of the cathode region where effective formation of OH radicals takes place.

Acknowledgment

This work is supported by China Scholarship Council (CSC) and by the Interuniversity Attraction Poles Program of the Belgian Science Policy (Project "PSI" - P6/08).

References

(1) Hayashi, D.; Hoeben, W.; Dooms, G.; van Veldhuizen, E.M.; Rutgers, W.R.; Kroesen, G.M.W. *Journal of Physics D-Applied Physics* **2000**, *33*, 2769-2774.

(2) Malik, M.A.; Ubaid ur, R.; Ghaffar, A.; Ahmed, K. *Plasma Sources Science & Technology* **2002**, *11*, 236-240.

(3) Gao, J.Z.; Liu, Y.J.; Yang, W.; Pu, L.M.; Yu, J.; Lu, Q.F. *Plasma Sources Science & Technology* **2003**, *12*, 533-538.

(4) Sunka, P. *Physics of Plasmas* **2001**, *8*, 2587-2594.

(5) Malik, M.A.; Ghaffar, A.; Malik, S.A. *Plasma Sources Science & Technology* **2001**, *10*, 82-91.

(6) Abou-Ghazala, A.; Katsuki, S.; Schoenbach, K.H.; Dobbs, F.C.; Moreira, K.R. *IEEE Transactions on Plasma Science* **2002**, *30*, 1449-1453.

(7) Sato, M.; Ohgiyama, T.; Clements, J.S. *IEEE Transactions on Industry Applications* **1996**, *32*, 106-112.

(8) Bruggeman, P. PhD thesis of Ghent University, 2009, p6, 149-151.

(9) Bruggeman, P.; Leys, C. *Journal of Physics D-Applied Physics* **2009**, *42*, 053001.

(10) Korobeinikov, S.M.; Melekhov, A.V.; Besov, A.S. *High Temperature* **2002**, 40, 652-659.

(11) Miichi, T. ; Ihara, S.; Satoh, S.; Yamabe, C.; *Vacuum* **2000**, *59*, 236-243.

(12) Kai-Yuan, S.; Locke, B.R. *Plasma Chemistry and Plasma Processing* **2010**, *30*, 1-20.

(13) Locke, B.R.; Shih, K.Y. *Plasma Sources Science & Technology* **2011**, *20*, 15.

(14) Grymonpre, D.R.; Sharma, A.K.; Finney, W.C.; Locke, B.R. Chem. Eng. J. **2001**, *82*, 189-207.

(15) Mededovic, S.; Locke, B.R. *Applied Catalysis B-Environmental* **2006**, *67*, 149-159.

(16) Nikiforov, A.Y.; Leys, C. *Plasma Sources Science & Technology* **2007**, *16*, 273-280.

(17) Nogueira, R.F.P.; Oliveira, M.C.; Paterlini, W.C. *Talanta* **2005,** *66*, 86-91.

(18) Nikiforov, A.Y.; Leys, C.; Li, L.; Nemcova, L.; Krema, F. *Plasma Sources, Science and Technology* **2011**, 034008 (034010 pp.).

(19) Nemcova, L.; Nikiforov, A.; Leys, C.; Krcma, F. *IEEE Transactions on Plasma Science* **2011**, *39*, 865-870.

(20) Mededovic, S.; Takashima, K.; Mizuno, A. *Plasma Chemistry and Plasma Processing* **2009**, *29*, 455-473.

(21) Shih, K.-Y.; Locke, B.R. *IEEE Transactions on Plasma Science* **2011**; *39*, 883-892.

(22) Bruggeman, P.; Jingjing, L.; Degroote, J.; Kong, M.G.; Vierendeels, J.; Leys, C. *Journal of Physics D: Applied Physics* **2008**, 215201 (215211 pp.).

(23) Bruggeman, P.; Leys, C.; Degroote, J.; Vierendeels, J. *In IEEE 35th International Conference on Plasma Science*, 2008.

(24) Wang, L. *Plasma Chemistry and Plasma Processing* **2009**, *29*, 241-250.

(25) Aristova, N.A.; Piskarev, I.M.; Ivanovskii, A.V.; Selemir, V.D.; Spirov, G.M.; Shlepkin, S.I. *Russian Journal of Physical Chemistry* **2004**, *78*, 1144-1148.

(26) Takagi, J.; Ishigure, K. *Nuclear Science and Engineering* **1985**, *89*, 177-186.

(27) Liu, D.X.; Bruggeman, P.; Iza, F.; Rong, M.Z.; Kong, M.G. *Plasma Sources Science & Technology* **2010**, *19*.

(28) Bruggeman, P.; Schram, D.C. *Plasma Sources Science & Technology* **2010**, *19*.

(29) Verreycken, T.; Schram, D.C.; Leys, C.; Bruggeman, P. *Plasma Sources Science & Technology* **2010**, *19*, 9.

(30) Sellers R.M. *Analyst* **1980**, *105*, 950-954.

(31) Bruggeman, P.; Schram, D.; Gonzalez, M.A.; Rego, R.; Kong, M.G; Leys, C. *Plasma Sources Science & Technology* **2009**, *18*, 2.

(32) Soloshenko, I.A; Tsiolko, V.V.; Pogulay, S.S.; Kalyuzhnaya, A.G.; Bazhenov, V.Y.; Shchedrin, A.I. *Plasma Sources Sci. Technol*. **2009,** *18*, 045019.

(33) Atkinson, R.; Baulch, D.L.; Cox, R.A.; Crowley, J.N.; Hampson, R.F.; Hynes, R.G.; Jenkin, M.E.; Rossi, M. ; Troe, J. *Atmos. Chem. Phys.* **2004**, *4*, 1461-738.

(34) NIST Chemical Kinetics Database, Standard Reference Database 17, Version 7.0 (Web Version), Release 1.4.2, Data Version 2009.01 (http://kinetics.nist.gov/kinetics/).

(35) Fridman, A; *Plasma Chemistry* (Cambridge: Cambridge University Press), 2008.

(36) Baulch, D.L.; Cox, R.A.; Hampson, R.F.; Kerr, J.A.; True, J.; Watson, R.T. *J. Phys. Chem. Ref. Data* **1980**, *9*, 295.

(37) Andre, P., et al. *Journal of Physics D-Applied Physics* **2001**, *34*(24), 3456-3465.

(38) Bruggeman, P., et al. *Journal of Physics D-Applied Physics* **2010**, *43*(1), 6.

(39) Mededovic, S.; Locke, B.R *Journal of Physics D Applied Physics* **2007,** *40*(24), 7734-7746.

(40) Mededovic, S.; Locke, B.R. *Industrial & Engineering Chemistry Research* **2007**, *46*(9), 2702-2709.

(41) XinPei, L.; Laroussi, M. *Journal of Physics D (Applied Physics)*, **2003**, *36*(6).

(42) XinPei, L.; Leipold, F.; Laroussi, M. *Journal of Physics D (Applied Physics)*, **2003**, *36*(21).

(43) Xinpei, L., et al., *Journal of Applied Physics* **2002**, *91*(1).

Received for review October 22, 2011. Revised manuscript received December 19, 2011. Accepted December 29, 2011.